Met Mutation is a Potential Therapeutic Target for Advanced Endometrial Cancer

Yu-Min Yeh
National Cheng Kung University Hospital
Pei-Ying Wu
National Cheng Kung University Hospital
Peng-Chan Lin
National Cheng Kung University Hospital
Pei-Fang Su
National Cheng Kung University
Ya-Ting Hsu
National Cheng Kung University Hospital
Jang-Yang Chang
National Health Research Institutes
Keng-Fu Hsu
National Cheng Kung University Hospital
Meng-Ru Shen (mrshen@mail.ncku.edu.tw)
Department of Obstetrics and Gynecology, National Cheng Kung University Hospital, College of Medicine, National Cheng Kung University, Taiwan;

Research

Keywords: endometrial cancer, MET mutation, germline variant, targeted therapy, chemoresistance

Posted Date: September 28th, 2020

DOI: https://doi.org/10.21203/rs.3.rs-80612/v1

Abstract

Background

An optimal therapeutic regimen for endometrial cancer with extra-uterine metastasis is unavailable. This study aimed to improve our understanding about the genomic landscape of advanced endometrial cancer and identify potential therapeutic targets.

Methods

The clinical and genomic profiles of 81 patients with stage III or IV endometrial cancer were integrated. The genomic landscape was compared with that of The Cancer Genome Atlas (TCGA) cohort. To identify genomic aberrations associated with clinical outcome, Cox proportional hazard regression was used. The impacts of the genomic aberrations were validated in vitro and in vivo.

Results

A discrepancy in major genetic aberrations that contributed to the genomic functions was observed between the present study and TCGA cohorts. The mutation status of *MET*, *U2AF1*, *BCL9*, *PPP2R1A*, *IDH2*, *CBL*, *BTK,* and *CHEK2* were positively correlated with poor clinical outcomes. *MET* mutations occurred in 30% of the patients who presented with poor overall survival (hazard ratio, 2.606; 95% confidence interval, 1.167~5.819; adjusted p-value, 0.067). Concurrent *MET* and *KRAS* mutations presented with the worst outcomes. *MET* mutations in HGF-binding (58.1%) or kinase (16.2%) domains resulted in differential HGF-induced c-MET phosphorylation. Different types of *MET* mutations differentially affected tumor growth and displayed different sensitivities to cisplatin and tyrosine kinase inhibitors. *MET* N375S mutation is a germline variant with a high incidence in Eastern Asia and causes chemoresistance to cisplatin.

Conclusions

This study highlights the ethnic differences in the biology of the disease, which can influence the treatment recommendations and the genome-guided clinical trials of advanced endometrial cancer.

Background

Endometrial cancer, the most common gynecological cancer in developed countries, is broadly classified into two types (type I and type II), based on its histology and the presence or absence of a hormone receptor.[1] Type I endometrioid cancer is associated with estrogen excess, obesity, hormone-receptor positivity, and a favorable prognosis, as compared to type II endometrial cancers, which present as serous tumors that are more common in non-obese women and exhibit a poorer outcome.[2] The 5-year overall survival rate ranges from 74–91% at the early stage (International Federation of Gynecology and Obstetrics, FIGO stages I or II). In contrast, the 5-year overall survival rates in patients with extra-uterine metastatic disease are 57–66% and 20–26% for FIGO stages III and IV, respectively.[3] Extra-uterine spread

is observed in about 25% of patients who are newly diagnosed with endometrial, and chemotherapy is the suggested mode of treatment. However, the optimal treatment of this cancer has not been determined so far. In general, platinum-based chemotherapy was used as the first-line treatment for metastatic or advanced endometrial cancer. However, no standard protocol for the second-line option when the tumor persists or recurs exists.[4]

The Cancer Genome Atlas (TCGA) Research Network produced a vast amount of data on the genomic landscape of endometrial cancer.[5] The genomic analysis categorized endometrial cancer into subgroups based on distinct molecular characteristics: the group with DNA polymerase epsilon (*POLE*) somatic mutations and the corresponding 'ultramutated' phenotype exhibit a favorable prognosis, while the other distinct subgroups, which include tumors with microsatellite instability, low copy number, and high copy number, consisted mostly of cases diagnosed as high-grade serous tumors with poor outcome. The treatment for metastatic disease is not well established, and the survival of patients with this disease has not improved over the last decade. No targeted therapy, except for hormonal therapy, has been approved so far.[6] Therefore, the identification of the biological pathways that may be altered in advanced endometrial cancer might aid in improving the clinical management of this disease.

This study aimed to identify the survival-associated molecular pathways in advanced endometrial cancer via integrated genomic characterization.

Methods

Study cohort. Patients with endometrial cancer were consecutively recruited at the National Cheng Kung University Hospital Taiwan from July 2006 to January 2017. About 900 patients with endometrial cancer were enrolled, and 20% of cases were diagnosed with advanced-stage cancer (FIGO stage III or IV). The patients received staging surgery or diagnostic dilation and curettage at initial diagnosis. Platinum plus paclitaxel were the standard regimens used as post-operative chemotherapy for patients with FIGO stage III and IV. The patients were recruited as an NCKUH cohort using the following inclusion criteria: (i) FIGO stage III or IV; (ii) surgery performed at NCKUH; and (iii) adequate and qualified specimens for genetic analysis. The exclusion criteria were as follows: (i) unavailable clinical information; (ii) death unrelated to cancer; and (iii) poor quality of specimens. This study was approved by the institutional review board of NCKUH (A-ER-103-151, A-ER-103-395, and A-ER-104-153). Whole-genome sequencing (WGS) data of 499 normal Taiwanese individuals were provided by the Taiwan Biobank as genome reference.

Next-generation sequencing. Genomic analysis was performed on formalin-fixed paraffin-embedded (FFPE) tumor tissues using Oncomine Comprehensive Assay™ v1 (ThermoFisher, MA, USA).[7] Hematoxylin and eosin (H&E)-stained FFPE sections were reviewed to ensure that the tumor content was > 50%. Genomic DNA and RNA were extracted from the sections using the Recover All Total Nucleic Acid Isolation Kit (Thermo Fisher Scientific). RNA was reverse-transcribed to produce cDNA using the SuperScript VILO cDNA Synthesis Kit (Thermo Fisher Scientific). Target regions from genomic DNA and cDNA were amplified using the DNA Oncomine Cancer Research and RNA Oncomine Cancer Research

panels (Thermo Fisher Scientific). Library construction of the amplicons was performed according to the manufacturer's instructions using the Ion AmpliSeq Library Kit 2.0 (Thermo Fisher Scientific). The template was prepared with the Ion PGM Template OT2 200 Kit (Thermo Fisher Scientific), and the Ion 318 chip (Thermo Fisher Scientific) was prepared and loaded according to the manufacturer's recommendations. The Ion PGM Sequencing 200 Kit v.2 (Thermo Fisher Scientific) was used with the Ion PGM sequencer (Thermo Fisher Scientific) as described in the User Guide (average sequencing depth, 1000×).

Next, *POLE* gene panels were designed and ordered at AmpliSeq.com to identify the pathogenic mutations in the gene. *POLE* gene libraries were prepared using the Ion AmpliSeq™ Kit for Chef DL8 with the Ion Chef™ System. Template preparation, chip loading, and sequencing were carried out on the Ion Chef™ System and Ion S5 XL sequencing system using the Ion 510 & Ion 520 & Ion 530 Kit-Chef Kit (Thermo Fisher Scientific). The sequencing reads were aligned to the reference genome (hg19), and variant calling and annotation were conducted using Ion Reporter Version 5.6.

To detect the germline genetic variant, DNA was isolated from the peripheral blood of 20 patients and adjacent non-tumor specimens of 15 patients. WGS and whole exome sequencing (WES) of the blood and tissue samples were performed using the Illumina HiSeq® 2500 and Ion Torren™ systems, respectively. NGS library preparation was carried out using the TruSeq PCR-Free DNA HT Library Prep kit (Illumina Inc). The size and concentration of the DNA library were measured using Agilent 2100 Bioanalyzer (Agilent) and Qubit Fluorometer (Life Technologies). WGS and WES were performed with a minimum median coverage of 30 × and 100×, respectively. FastQC was used to check the quality of the reads, which were aligned to the hg19 reference genome using the BWA-MEM algorithm. The GATK Best Practices was used for base quality score recalibration, small insertion and deletion (INDEL) realignment, and duplicate removal.[8] Single nucleotide variant (SNV) and INDEL discovery and genotyping were performed according to GATK.[9,10] Manta and Canvas were used for SNV and CNV discovery.[11,12] To study the possible functional impacts of the associated variants, the Ensemble Variant Effect Predictor was used.[13]

Site-directed mutagenesis of MET. The pCMV6-MET mutant (N375S) plasmid was purchased from ORIGENE (#RC400336). The construction of mutated derivatives of *c-MET* was performed using the QuikChange site-directed mutagenesis kit (Agilent Technologies). Mutations for target nucleotide were introduced using the designed oligonucleotides and pCMV6-MET (ORIGENE; #RC217003) as a template. The PCR products were added to DpnI enzyme for 5 min at 37 °C to destroy the parental plasmid DNA and then transformed into *E. coli*. All mutated constructs were confirmed by sequencing.

Cell culture and functional assays. In April 2017, authenticated endometrial cancer cell lines, RL95-2 and KLE, were purchased from the American Type Culture Collection. Cell functions on proliferation, migration, and invasion were performed as previously described[14]. Briefly, the RL95-2 and KLE cell lines transfected with wild-type and mutant *c-MET* were seeded into 96-well plates (5×10^3/ well) with 100 µl of culture medium and incubated at 37ºC with 5% CO_2. Cell proliferation was evaluated 0, 24, 48, and 72 h after

seeding using the Alamar Blue assay (Invitrogen). Next, transwell assay was used to evaluate the migration and invasion abilities of the transfected cells. For the invasion assay, 100 µl of matrigel (10%; BD Biosciences) was added to the bottom of the transwell insert. Next, 3×10^4 transfected cells were seeded on to the transwell insert along with 300 µl of medium containing 5% FBS; 1 ml of medium with 10% FBS was added to the lower part of the 24-well plate. The cells were allowed to invade or migrate for 24 h at 37 °C with 5% CO_2. All the cells from the underside of the transwell inserts were stained by crystal violet. Images of each transwell insert were taken to count the number of cells.

c-MET phosphorylation. The cells were washed with phosphate-buffered saline (PBS) and lysed in cell lysis buffer (10 mM Tris pH7.4, 150 mM NaCl, 1 mM ethylenediaminetetraacetic acid [EDTA], 1% octylphenoxypolyethoxyethanol (IGEPAL), 0.5% deoxycholic acid, and 0.1% SDS) containing freshly added Protease Inhibitor Cocktail (Sigma, St Louis, MO, USA) and 1 mM phenylmethanesulfonylfluoride (PMSF). The protein concentration of the cell lysate was determined using the DC Protein Assay (Bio-Rad Laboratories, Hercules, CA, USA). Equal amounts of lysate protein (30 µg) from each cell lysate were loaded on to 4–15% SDS-polyacrylamide gel (Bio-Rad) and separated by electrophoresis. The separated proteins were electroblotted onto a nitrocellulose membrane (0.45 µm; Bio-Rad) and incubated in blocking solution (1X PBS, 0.1% Tween-20, 5% non-fat dry milk powder) for 1 h at room temperature. The membranes were incubated with the following dilutions of the primary antibody at 40 °C overnight: anti-phospho-c-MET, 1:1,000 (#3077; Cell Signaling Technology); anti-c-MET, 1:2,000 (#8198; Cell Signaling Technology); and anti-α-tubulin, 1:5,000 (DM1A; Novus Biologicals). After multiple washes with PBS containing 0.1% Tween-20 (PBST), the membranes were incubated with horseradish peroxidase-conjugated secondary antibody (goat anti-mouse or goat anti-rabbit IgG; Bio-Rad) for 1 h at room temperature. After further washes with PBST, the membranes were processed using the enhanced chemiluminescence method (SuperSignal West Pico substrate; Pierce, Rockford, IL, USA). Protein bands were visualized by autoradiography, and the signal intensities were quantified by using the NIH ImageJ software.

Immunohistochemical staining. FFPE endometrial cancer tissues from surgical specimens were used to determine the expression of c-MET protein. Tissue sections were cut from the paraffin block (thickness, 4 µm), deparaffinized in xylene, and rehydrated with decreasing grades of ethanol. Immunohistochemical staining for the MET protein was performed using the anti-MET rabbit polyclonal antibody (sc-161; Santa Cruz Biotechnology). The expression level of MET in tumors with wild-type *c-MET* was compared with those in tumors carrying various *c-MET* mutations.

In silico **analysis.** To predict the effect of variants on the function of the c-MET protein, differences in free energy between mutant and wild-type *MET* were calculated using Calculate Mutation Energy.[24] For the variants located in the tyrosine kinase domain, the analysis was performed using the crystal structure of the kinase domain in complex with ATP. Regarding the variants located in the Sema domain, the binding with HGF was used for estimation. Variants with mutation energy higher than 0.5 kcal/mol were reported as destabilized.

Animal Study. All animal experiments were approved by the Laboratory Animal Care and Use Committee of the NCKU. The xenograft procedures were performed in 6–8-week-old, female, severe combined immunodeficient (NOD.CB18-Prkdc^{scid}/JNarl, NOD/SCID) mice. The posterior flank of the NOD-SCID mouse was subcutaneously inoculated with 1×10^6 endometrial cancer RL95-2 cells expressing either wild-type or mutant *MET* (N375S, G1085R, G1087E). The mice were randomly divided into four groups (at least four mice in each group) and treated with cisplatin, crizotinib (multiple tyrosine kinase inhibitor), SU11274 (a specific c-MET inhibitor), or none of the aforementioned drugs; the treatments were initiated 1 week after tumor inoculation. Cisplatin (1 mg/kg) and SU11274 (6 mg/kg) were administered twice a week via intraperitoneal (i.p.) injection for 5 weeks. Crizotinib (25 mg/kg), prepared with 0.5% hydroxypropylmethylcellulose, was administered by oral gavage twice a week for 5 weeks. Both tumor size and body weight were measured twice a week, and tumor volume was determined via caliper measurements of the tumor length (L) and width (W) according to the following formula: $LW^2/2$. The mice were sacrificed at day 40, and the tumors were excised and weighed.

Statistics. Chi-Square test, Fisher's exact test, and unpaired *t*-test were used to compare the differences between the groups. After adjusting for the stage of the tumor, the association between individual mutated gene and survival outcome was assessed using the Cox proportional hazards regression model. The correction for multiple comparisons was performed using the False Discovery Rate (FDR) method. The cutoff for the FDR adjusted *p*-value was 0.1. Kaplan-Meier curves and log-rank tests were used to estimate the survival functions and compare the differences between groups. A p-value of < 0.05 was considered statistically significant.

Results

Patient characteristics. Eighty-one patients with stage III and IV cancer were consecutively recruited based on the inclusion criteria. The clinical characteristics of the patients were shown in Supplementary Table S1. Based on the histology, 80% and 20% of the patients presented with Type I (mainly endometrioid) and Type II (non-endometrioid) tumors, respectively. Furthermore, the patients were grouped based on the clinical outcome as follows (Table 1): no evidence of disease and progressive disease (PD). The clinical characteristics of the patients in the two groups are shown in Table 1. No significant differences in histology, grading, and treatment were observed between the two groups of patients.

Table 1
Patient characteristics

Characteristics	No evidence of disease (N = 47)	Progressive disease or death (N = 34)	*P*
Age (years)			0.5287
Mean (range)	53.2 (34 ~ 76)	58.8 (34 ~ 87)	
FIGO staging			<0.001
Stage III	44 (93.6%)	18 (52.9%)	
Stage IV	3 (6.4%)	16 (47.1%)	
Histology			0.151
Endometrioid	41 (87.2%)	24 (70.6%)	
Others	6 (12.8%)	10 (29.4%)	
Grading*			0.078
1	10	3	
2	23	13	
3	14	18	
Survival (months)			
Progression-free survival	48.4 (1.7 ~ 119.1)	14.8 (1.7 ~ 75.5)	<0.0001
Overall survival	48.4 (1.7 ~ 119.1)	23.9 (1.7 ~ 92.5)	<0.002
Treatment			
Staging surgery	47	31	0.834
Others[#]	0	3	
Chemotherapy	46	34	0.853
*Pathological grading: clear cell carcinoma, serous carcinoma, and carcinosarcoma were classified as grade 3			
[#]Others: dilatation & curettage for diagnosis alone			

Clinical impacts of gene mutation. The Oncomine Comprehensive Assay v1, a targeted NGS assay, was applied to the FFPE tumor samples to detect the presence of mutations across 143 genes. Associations between the individual mutated gene and the clinical outcome with FDR adjusted p-value < 0.1 are shown

in Tables 2 and 3. The mutation status of eight genes (*MET*, *U2AF1*, *BCL9*, *PPP2R1A*, *IDH2*, *CBL*, *BTK*, and *CHEK2*) were positively correlated with poor progression-free survival (PFS) and overall survival (OS). In contrast, *IFITM1* and *DNMT3A* mutations were associated with better clinical outcomes. *MET* was selected for further studies because the adjusted p-value was the smallest and the frequency of mutation was not low.

Table 2
The association between the mutated genes and overall survival.

Gene	Case number with mutation	Case number without mutation	p value	Adjusted p value	Hazard ratio	95% interval (Lower ~ Upper)
MET	24	57	0.019	0.067	2.606	1.167–5.819
U2AF1	3	78	0.006	0.067	5.942	1.683 ~ 20.980
BCL9	4	77	0.022	0.067	4.343	1.241 ~ 15.201
PPP2R1A	8	73	0.020	0.067	3.272	1.204 ~ 8.892
IFITM1	79	2	0.018	0.067	0.151	0.031 ~ 0.724
IDH2	2	79	0.018	0.067	6.44	1.381 ~ 30.036
EGFR	7	74	0.041	0.088	2.785	1.040 ~ 7.457
CBL	2	79	0.039	0.088	4.856	1.086 ~ 21.703
DNMT3A	9	72	0.049	0.088	0.222	0.049 ~ 0.995
BTK	2	79	0.039	0.088	4.856	1.086 ~ 21.703
RB1	21	60	0.079	0.094	2.012	0.923 ~ 4.382
CHEK2	4	77	0.067	0.094	3.215	0.921 ~ 11.230
MLH1	14	67	0.077	0.094	2.216	0.918 ~ 5.348
PIK3R1	37	44	0.065	0.094	2.113	0.954 ~ 4.680
ESR1	2	79	0.058	0.094	7.715	0.937 ~ 63.546
KRAS	37	44	0.068	0.094	2.059	0.949 ~ 4.469
FGFR3	7	74	0.083	0.094	2.621	0.882 ~ 7.792
GNAQ	3	78	0.089	0.097	3.749	0.818 ~ 17.190
NKX2_1	3	78	0.098	0.098	3.615	0.790 ~ 16.551
CCNE1	5	76	0.097	0.098	2.572	0.843 ~ 0.098

Table 3
The association between the mutated genes and progression-free survival.

Gene	Case number with mutation	Case number without mutation	p value	Adjusted p value	Hazard ratio	95% interval (Lower ~ Upper)
MET	24	57	0.044	0.067	2.081	1.020 ~ 4.248
BCL9	4	77	0.059	0.067	3.274	0.958 ~ 11.194
TSC2	27	54	0.029	0.067	2.122	1.079 ~ 4.177
NF1	48	33	0.052	0.067	2.222	0.993 ~ 4.974
MAP2K2	2	79	0.063	0.067	4.066	0.926 ~ 17.854
NFE2L2	6	75	0.062	0.067	0.244	0.056 ~ 1.073
U2AF1	3	78	0.008	0.067	5.395	1.563 ~ 18.615
CHEK2	4	77	0.049	0.067	3.503	1.007 ~ 12.184
VHL	8	73	0.020	0.067	3.293	1.206 ~ 8.993
CBL	2	79	0.016	0.067	6.589	1.425 ~ 30.475
IFITM1	79	2	0.023	0.067	0.168	0.036 ~ 0.778
IDH2	2	79	0.049	0.067	4.398	1.005 ~ 19.250
DNMT3A	9	72	0.036	0.067	0.267	0.078 ~ 0.918
BTK	2	79	0.016	0.067	6.589	1.425 ~ 30.475
PPP2R1A	8	73	0.087	0.087	2.329	0.883 ~ 6.143

MET **mutation is a cancer driver.** *MET* mutation is a poor clinical marker (Fig. 1A). c-MET, a protein encoded by the human *MET* gene, is a receptor tyrosine kinase (RTK) expressed on the cell surface (1). The aberrant activation of the c-MET pathway and crosstalk with other RTKs has been shown to stimulate the PI3K/AKT and RAS/MAPK signaling pathways, which contribute to cancer biology (Supplementary Fig. 1A). *MET* mutation was associated with poor survival independent of *EGFR* mutation (Supplementary Fig. 1B). Alternatively, *EGFR* mutation did not affect the clinical outcome in patients harboring the wild-type or mutant *MET*. Similar results were observed in the *MET* and *ERBB2*, *MET* and *PIK3R1*, and *MET* and *PIK3CA* combination mutations (Supplementary Fig. 1C, Figs. 1B and 1C). However, the impacts of *KDR* and *KRAS* mutations were different. The presence of *KDR* or *KRAS* mutations indicated poor outcomes in patients with *MET* mutations, but not in those without *MET* mutations (Supplementary Fig. 1D and Fig. 1D). Taken together, *MET* mutation highly influences the clinical outcome of advanced endometrial cancer, and *KDR* and *KRAS* mutations exhibit additional impacts on patients with *MET* mutation.

In silico **analysis of** MET **mutation.** The types of *MET* mutations were analyzed in 112 samples, including 81 primary tumors and 31 metastatic tissues. A total of 35 nonsynonymous mutations, including missense mutations and small INDELs, were identified in exons 2, 10, 11, 14, 15, and 16 (Fig. 2A, Supplementary Figure S2A). Aberrant *MET* mutations resulted in c-MET overexpression in the endometrial cancer tissues (Fig. 2B), similar to that seen in lung cancer, indicating that c-MET overexpression alone can induce oncogenic transformation *in vitro* and *in vivo.* [16,17,18,19] Moreover, patients with intracellular domain mutations seemed to exhibit a worse outcome (Supplementary Figure S2B).

To predict the impact of the *MET* mutations on the protein structure, the *"in silic*o" analysis was performed.[20] When the interaction between the semaphorin domain of c-MET and HGF was analyzed (Supplementary Figure S3A), the exon 2 mutations in did not cause any obvious change in the predicted free energy, implying that these mutations did not theoretically affect the binding of HGF to c-MET (Supplementary Figure S3B). For mutations in the kinase domain, the free energy changes were studied in the presence of ATP (Supplementary Figure S3C). As shown in Supplementary Figure S3D, the "*in silico"* models demonstrated a Gly-to-Arg or Gly-to-Glu change at codon 1085 or a Gly-to-Glu change at codon 1087, which increased the mutational free energy. These findings indicated that these mutations might affect ATP binding, c-MET phosphorylation, and subsequent biological functions.

Effect of MET **mutation on cellular function.** To confirm the "*in silico"* analysis, we established various clones of *MET* mutants in the RL95-2 and KLE cell lines. The time course of c-MET phosphorylation was studied in response to HGF stimulation. In the wild-type c-MET RL95-2 cells, HGF induced a rapid increase in c-MET phosphorylation within 3 min, which was gradually decreased over 120 min (Fig. 2C). In contrast, an equivalent increase in c-MET phosphorylation was observed, which was sustained for 120 min in exons 15 (G1085E) or 16 (G1087E) in the clones of the kinase domain mutants. In the mutated semaphorin domain N375S clones, a delayed peak in c-MET phosphorylation was noted at 30 min, followed by rapid dephosphorylation. These results imply that different *MET* aberrations might exert differential effects on cellular functions. This hypothesis was confirmed by the proliferation, migration, and invasion assays in the endometrial cancer cell lines (Fig. 2D & 2E, Supplementary Figure S4).

Endometrial cancer growth in vivo. To test whether the c-MET signaling pathway was a therapeutic target, we subcutaneously inoculated the SCID mice with RL95-2 cells carrying various *MET* mutations. Tumors harboring different *MET* mutants showed a significant increase in volume when compared to those with wild-type *MET* (Fig. 3A-B, Supplementary Figure S5). Next, cisplatin significantly inhibited the growth of tumors carrying the wild-type *MET* and the G1085R and G1087E mutations (Fig. 3C-D). However, it appeared to exhibit no inhibitory effect on tumors with *MET* N375S. Crizotinib, a multi-target tyrosine kinase inhibitor, significantly inhibited the growth of tumors carrying the N375S, G1085R or G1087E mutant, when compared to those with the wild-type *MET* (Fig. 3E-F). SU11274, a specific c-MET inhibitor, also showed potent inhibitory effects on the growth of tumors carrying G1085R or 1087E mutations, whereas its inhibitory effect on the growth of tumors carrying wild-type *MET* was not very obvious. Interestingly, tumors with N375S mutation were insensitive to SU11274 *in vivo* (Fig. 3G-H). These data

indicate that *MET* mutations promote the growth of endometrial tumors and show different sensitivities to cisplatin or tyrosine kinase inhibitors (crizotinib and SU11274), depending on the type of *MET* mutation.

MET **N375S is a germline variant.** In animal studies, mutation of the semaphorin domain N375S displayed resistance to cisplatin, the major chemotherapeutic agent for endometrial cancer (Fig. 3C and D). In our cohort, the OS rate for patients without *MET* mutations was 75%; however, that value significantly decreased to 50% in patients with *MET* N375S (Fig. 4A, P = 0.043). Furthermore, an analysis of 35 paired tissues revealed that the *MET* N375S mutation was a germline variant (Fig. 4B), consistent with the findings of a previous study in lung cancer.[21] When compared to other nonsynonymous variants, the incidence of the N375S variant (c.1124 A > G) was relatively high (11 ~ 17%) in the current study and the Taiwan Biobank (Fig. 4C). The worldwide distribution of genetic N375S variants (c.1124 A > G) was assessed in the data from the 1000 Genomes Project. The allele frequency of the *MET* N375S variant (c.1124 A > G) was 8.5% and 5.8% in all the patients enrolled in the present study and the Taiwan Biobank, respectively. A similar allele frequency (5%~8%) was observed in the population from South and East Asia (Fig. 4D). In contrast, less than 2% of the alternative allele frequency was observed in the European, American, and African populations.

Comparison with TCGA molecular classification. Patients with advanced disease (stage III or IV) in the TCGA endometrial cancer cohort were identified, and the genomic backgrounds between the NCKUH and TCGA cohort were compared. No significant differences in age distribution at initial diagnosis, FIGO stage, histology, and clinical outcome were observed between the two cohorts (Supplementary Figure S6A and S6B). To obtain somatic mutations, the variants identified by Oncomine Comprehensive Assay v1 were filtered by the germline genetic variants. The top gene aberrations with high impact on genomic functions were listed after analyzing and filtering out the mutations, which were categorized as “low” (harmless or unlikely to change protein behavior), “modifier” (affecting the non-coding), or “moderate” (inframe insertion or protein-altering variant; Supplementary Figure S6C). The ranking of the top 10 genetic aberrations was different between the two cohorts, although *PTEN* was the most common mutated gene. Mutations in *BRAF*, *JAK1*, and *KIT* were identified in approximately 4–11% of the patients in TCGA cohort, but they were rarely detected in the NCKUH cohort. In addition, at the advanced stage, *MET* mutations were observed in 15% of cases in the TCGA cohort without an impact on the OS (Supplementary Figure S6D).

A subset of endometrioid cancer was newly identified in hotspot *POLE* mutations in the TCGA cohort.[5] TCGA and subsequent studies showed that *POLE*-mutant endometrial cancers typically present as high-grade or poorly-differentiated tumors.[5,22] In addition, *POLE* mutations accompanied by an ultra-tumor mutation burden present with favorable clinical outcomes.[5,23] Among the 81 patients recruited in this study, 74 presented with adequate and qualified samples to investigate the pathogenic mutations in the *POLE* gene. However, no association between the *POLE* mutation and the histology of the specimens was observed in the current study cohort (Supplementary Figure S7A). In addition, the OS was not affected by

the presence of the *POLE* mutation (Supplementary Figure S7B). A discrepancy in the genetic aberrations between the NCKUH and TCGA cohorts was noted.

Discussion

This study highlights the survival-associated molecular pathways in advanced endometrial cancer. *MET* mutation was found to be a potential therapeutic target. This conclusion was reached based on several important findings. First, the *MET* mutation was noted in 30% of the advanced endometrial cancer cases and was associated with a poor clinical outcome; concurrent *MET* and *KRAS* mutations indicated the worst outcome. Second, *MET* mutation promoted the growth and invasion of endometrial tumors both in vivo and in vitro. Third, *MET* mutation occurred in the HGF-binding or kinase domain. Mutations in the kinase domain induce sustained c-MET phosphorylation in response to HGF stimulation. Consistently, patients with kinase domain mutations presented with the worst clinical outcome compared to those with mutations in extracellular regions. Fourth, tumors harboring c-MET kinase domain mutations in the SCID mouse model were sensitive to the tyrosine kinase inhibitors and cisplatin. Finally, mutation of the Sema domain N375S provided resistance against cisplatin, and this effect was not overcome by the selective c-MET inhibitor.

The HGF-MET signaling pathway regulates cell proliferation and motility.[16,17] The Sema domain of c-MET is necessary for HGF-binding, receptor dimerization, and the activation of the downstream signaling. In the present study, 58% of the *MET* mutations were identified in the Sema domain, and N375S was the most frequent mutation within this region. An analysis of the paired genomic DNA in normal and tumor tissues and in the data obtained from the 1000 Genome Projects revealed that *MET* N375S mutation was a germline variant with high frequency in the Asian population. This ethnic difference was previously reported in patients with lung cancer, and *MET* N375S was reported to confer resistance to c-MET inhibition.[21] Earlier studies suggested that the resistance to c-MET inhibitor was caused by a missense change in the 375 serine residue, leading to a weakening in the interaction between HGF and c-MET and a decrease in kinase activation, thereby resulting in increased resistance to the c-MET inhibitor.[24,25] This notion was supported by our experiments in the endometrial cancer cell line, which showed that HGF induced delayed c-MET phosphorylation accompanied by rapid dephosphorylation. In the SCID mouse models, tumors harboring *MET* N375S were consistently resistant to the specific c-MET inhibitor, SU11274.

Interestingly, *MET* N375S provided drug resistance to cisplatin in the mouse model, in the current study. Cisplatin is one of the most active chemotherapeutic agents used in endometrial cancer. The poor clinical outcome in patients with *MET* N375S mutation in the NCKUH cohort supported this important finding in vivo. To the best of our knowledge, this correlation with chemoresistance has not been reported so far. Given the nature of the germline genetic variant, N375S would be a “de novo” mechanism of cisplatin resistance. The selection of patients based on the germline *MET* genetic variant may prove more beneficial for patients with endometrial cancer receiving cisplatin-based therapy and could be a new therapeutic strategy in precision medicine.

A discrepancy in the genetic aberration, in terms of the severity of the effect of the mutation on genomic functions, was observed between the current study cohort and TCGA cohort. In TCGA cohort, *POLE*-mutant endometrial cancers were typically high-grade or poorly-differentiated.[5] *POLE* mutations accompanied by ultra-tumor mutation burden presented with a favorable clinical outcome.[23] Conversely, in our cohort, the results showed no associations between *POLE* mutation, histologic subtype, and clinical outcome.

Conclusions

This integrated genomic and mechanistic study provides insights into the biology and diagnostic classification of advanced endometrial cancer, which might result in a direct effect on the treatment recommendations for patients with this disease. Furthermore, this information provides opportunities for additional genome-guided clinical trials and drug development. Since several c-MET inhibitors are FDA-approved drugs and in the late phases of the clinical trials, the next step is to launch a clinical trial intended at targeting *MET* mutations in advanced endometrial cancers.

Abbreviations

BWA-MEM
Burrows-Wheeler Aligner-Maximal Exact Matches
CMV
Cytomegalovirus
CNV
Copy Number Variation
DNA
Deoxyribonucleic Acid
EDTA
Ethylenediaminetetra-Acetic Acid
FDR
False Discovery Rate
FIGO
The International Federation of Gynecology and Obstetrics
GATK
Genome Analysis Tool Kit
INDEL
Insertion and Deletion
MAPK
Mitogen-Activated Protein Kinase
NIH
National Institutes of Health

OS
Overall Survival
PBS
Phosphate-Buffered Saline
PCR
Polymerase Chain Reaction
PFS
Progression-Free Survival
PMSF
Phenylmethanesulfonylfluoride
POLE
DNA Polymerase Epsilon
RNA
Ribonucleic Acid
SCID
Severe Combined Immunodeficient
SDS
Sodium Dodecyl Sulfate
SNV
Single Nucleotide Variant
TCGA
The Cancer Genome Atlas
WES
Whole Exome Sequencing
WGS
Whole-Genome Sequencing
FFPE
Formalin-Fixed Paraffin-Embedded

Declarations

Ethics approval and consent to participate

This clinical study was approved by the institutional review board (IRB) of NCKUH (A-ER-103-151, A-ER-103-395, and A-ER-104-153) and all participants provided written informed consent. Animal studies were approved by the Institutional Laboratory Animal Care and Use Committee (IACUC) of the NCKU.

Consent for publication

Not applicable.

Availability of data and materials

The datasets used and/or analyzed during the current study are available from the corresponding author on reasonable request.

Competing interests

The authors declare that they have no competing interests.

Funding

This study was supported by the Ministry of Science and Technology, Ministry of Health and Welfare (MOHW109-TDU-B-211-134018) and National Health Research Institutes (NHRI-109A1-CACO-02202011).

Authors' contributions

Conception and study design: Y.M. Yeh, P.Y. Wu, K.F. Hsu, and M.R. Shen; Methodology: Y.M. Yeh and P.Y. Wu; Acquisition and interpretation of data: Y.M. Yeh, P.Y. Wu, P.C Lin, Y.T. Hsu, and J.Y. Chang; Statistical analysis: P.F. Su; Writing, review, and revision of the manuscript: Y.M. Yeh, P.Y. Wu, K.F. Hsu, and M.R. Shen; Administrative and material support: P.C Lin, Y.T Hsu and J.Y. Chang; Study supervision: M.R. Shen and K.F. Hsu

Acknowledgments

We thank the bioinformatics support from Kimforest LTD Taiwan and also appreciate the help of Dr. Chin-Han Wu in animal studies.

References

1. Ferlay J, Soerjomataram I, Dikshit R, Eser S, Mathers C, Rebelo M, et al. Cancer incidence and mortality worldwide: sources, methods and major patterns in GLOBOCAN 2012. Int J Cancer. 2015;136:E359-86.
2. Lax SF, Kurman RJ. A dualistic model for endometrial carcinogenesis based on immunohistochemical and molecular genetic analyses. Verh Dtsch Ges Pathol. 1997;81:228–32.
3. Lewin SN, Herzog TJ, Barrena Medel NI, Deutsch I, Burke WM, Sun X, et al. Comparative performance of the 2009 international Federation of gynecology and obstetrics' staging system for uterine corpus cancer. Obstet Gynecol. 2010;116:1141–9.
4. National Comprehensive Cancer Network. Website https://www.nccn.org/.
5. Cancer Genome Atlas Research Network. Kandoth C, Schultz N, Cherniack AD, Akbani R, Liu Y, et al. Integrated genomic characterization of endometrial carcinoma. Nature. 2013; 497:67–73.
6. Aghajanian C, Filiaci V, Dizon DS, Carlson JW, Powell MA, Secord AA, et al. A phase II study of frontline paclitaxel/carboplatin/bevacizumab, paclitaxel/carboplatin/temsirolimus, or ixabepilone/carboplatin/bevacizumab in advanced/recurrent endometrial cancer. Gynecol Oncol. 2018;150:274–81.

7. Hovelson DH, McDaniel AS, Cani AK, Johnson B, Rhodes K, Williams PD, et al. Development and validation of a scalable next-generation sequencing system for assessing relevant somatic variants in solid tumors. Neoplasia. 2015;17:385–99.
8. Aaron M, Matthew H, Eric B, Andrey S, Kristian C, Andrew K, et al. The Genome Analysis Toolkit: a MapReduce framework for analyzing next-generation DNA sequencing data. Genome Res. 2010;20:1297–303.
9. DePristo MA, Banks E, Poplin R, Garimella KV, Maguire JR, Hartl C, et al. A framework for variation discovery and genotyping using next-generation DNA sequencing data. Nat Genet. 2011;43:491–8.
10. Van der Auwera GA, Carneiro MO, Hartl C, Poplin R, Del Angel G, Levy-Moonshine A, et al. From FastQ data to high confidence variant calls: the Genome Analysis Toolkit best practices pipeline. Curr Protoc Bioinformatics. 2013;43:11.10.1–33.
11. Chen X, Schulz-Trieglaff O, Shaw R, Barnes B, Schlesinger F, Källberg M, et al. Manta: rapid detection of structural variants and indels for germline and cancer sequencing applications. Bioinformatics. 2016;32:1220–2.
12. Roller E, Ivakhno S, Lee S, Royce T, Tanner S. Canvas: versatile and scalable detection of copy number variants. Bioinformatics. 2016;32:2375–7.
13. McLaren W, Gil L, Hunt SE, Riat HS, Ritchie GR, Thormann A, et al. The ensembl variant effect predictor. Genome Biol. 2016;17:122.
14. Chen YF, Chen LH, Shen MR. The distinct role of STIM1 and STIM2 in the regulation of store-operated Ca^{2+} entry and cellular function. J Cell Physiol. 2019;234:8727–39.
15. Chen YF, Chiu WT, Chen YT, Lin PY, Huang HJ, Chou CY, et al. Calcium store sensor stromal-interaction molecule 1-dependent signaling plays an important role in cervical cancer growth, migration, and angiogenesis. Proc Natl Acad Sci USA. 2011;108:15225–30.
16. Gherardi E, Birchmeier W, Birchmeier C, Vande Woude G. Targeting MET in cancer: rationale and progress. Nat Rev Cancer. 2012;12:89–103.
17. Cortot AB, Kherrouche Z, Descarpentries C, Wislez M, Baldacci S, Furlan A, et al. Exon 14 deleted MET receptor as a new biomarker and target in cancers. J Natl Cancer Inst. 2017;109.
18. Goździk-Spychalska J, Szyszka-Barth K, Spychalski L, Ramlau K, Wójtowicz J, Batura-Gabryel H, et al. C-MET inhibitors in the treatment of lung cancer. Curr Treat Options Oncol. 2014;15:670–82.
19. Ye S, Li J, Hao K, Yan J, Zhou H. The efficacy and risk profile of c-Met inhibitors in non-small cell lung cancer: a meta-analysis. Sci Rep. 2016;6:35770.
20. Spassov VZ, Yan L. pH-selective mutagenesis of protein-protein interfaces: in silico design of therapeutic antibodies with prolonged half-life. Proteins. 2013;81:704–14.
21. Krishnaswamy S, Kanteti R, Duke-Cohan JS, Loganathan S, Liu W, Ma PC, et al. Ethnic differences and functional analysis of MET mutations in lung cancer. Clin Cancer Res. 2009;15:5714–23.
22. McAlpine J, Leon-Castillo A, Bosse T. The rise of a novel classification system for endometrial carcinoma; integration of molecular subclasses. J Pathol. 2018;244:538–49.

23. Church DN, Stelloo E, Nout RA, Valtcheva N, Depreeuw J, Ter Haar N, et al. Prognostic significance of POLE proofreading mutations in endometrial cancer. J Natl Cancer Inst. 2015;107:402.
24. Sattler M, Reddy MM, Hasina R, Gangadhar T, Salgia R. The role of the c-Met pathway in lung cancer and the potential for targeted therapy. Adv Med Oncol. 2011;3:171–84.
25. Shieh JM, Tang YA, Yang TH, Chen CY, Hsu HS, Tan YH, et al. Lack of association of C-Met-N375S sequence variant with lung cancer susceptibility and prognosis. Int J Med Sci. 2013;10:988–94.

Figures

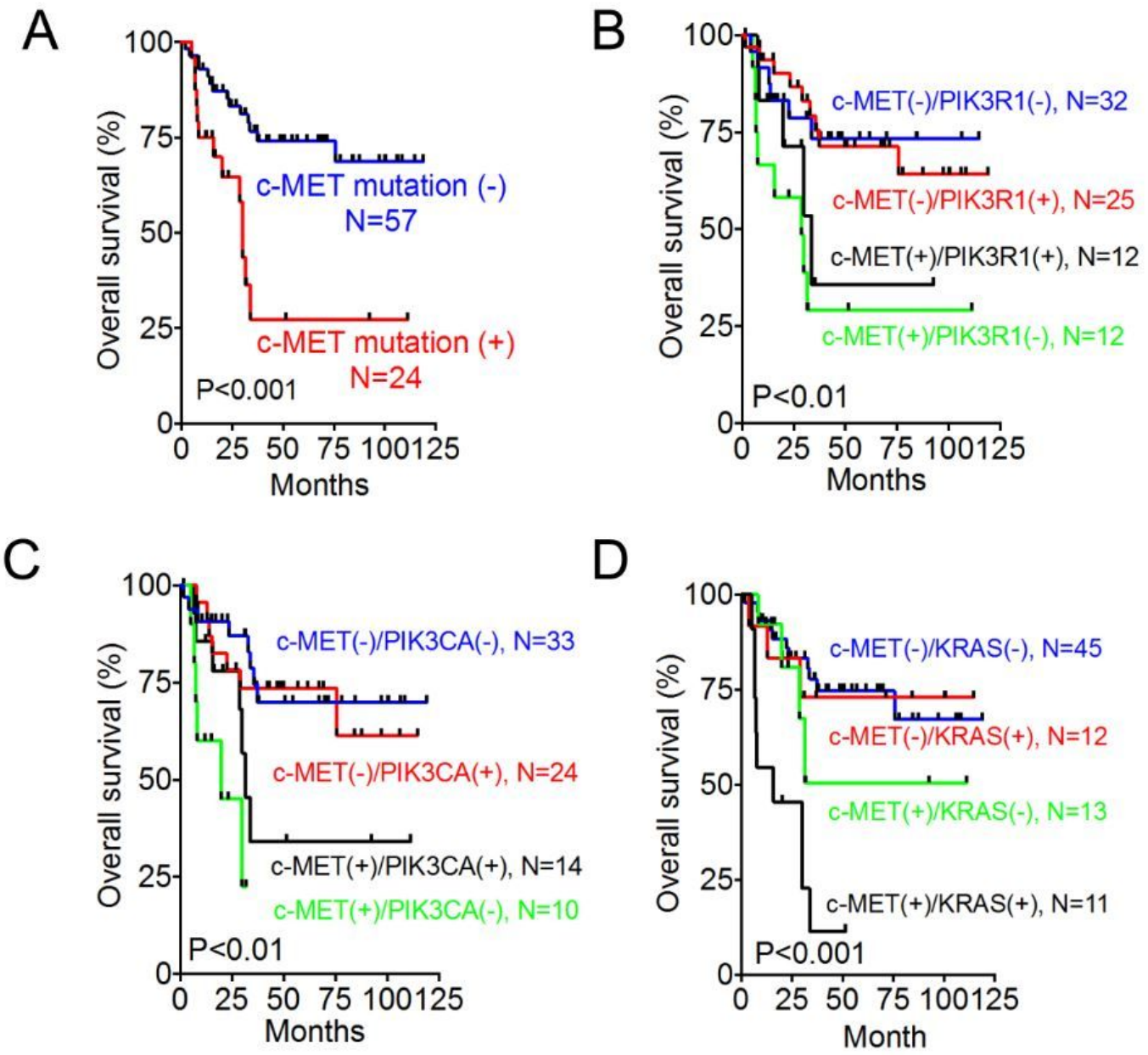

Figure 1

Impact of MET mutation and concurrent genetic mutations on the clinical outcome of advanced endometrial cancer. (A) Kaplan-Meier curves for overall survival (OS) in patients with and without MET mutation compared using the log-rank test. (B~D) Kaplan-Meier curves for OS were analyzed between the MET wild-type and MET mutant patients with or without concurrent PIK3R1 (B), PIK3CA mutation (C), and KRAS (D).

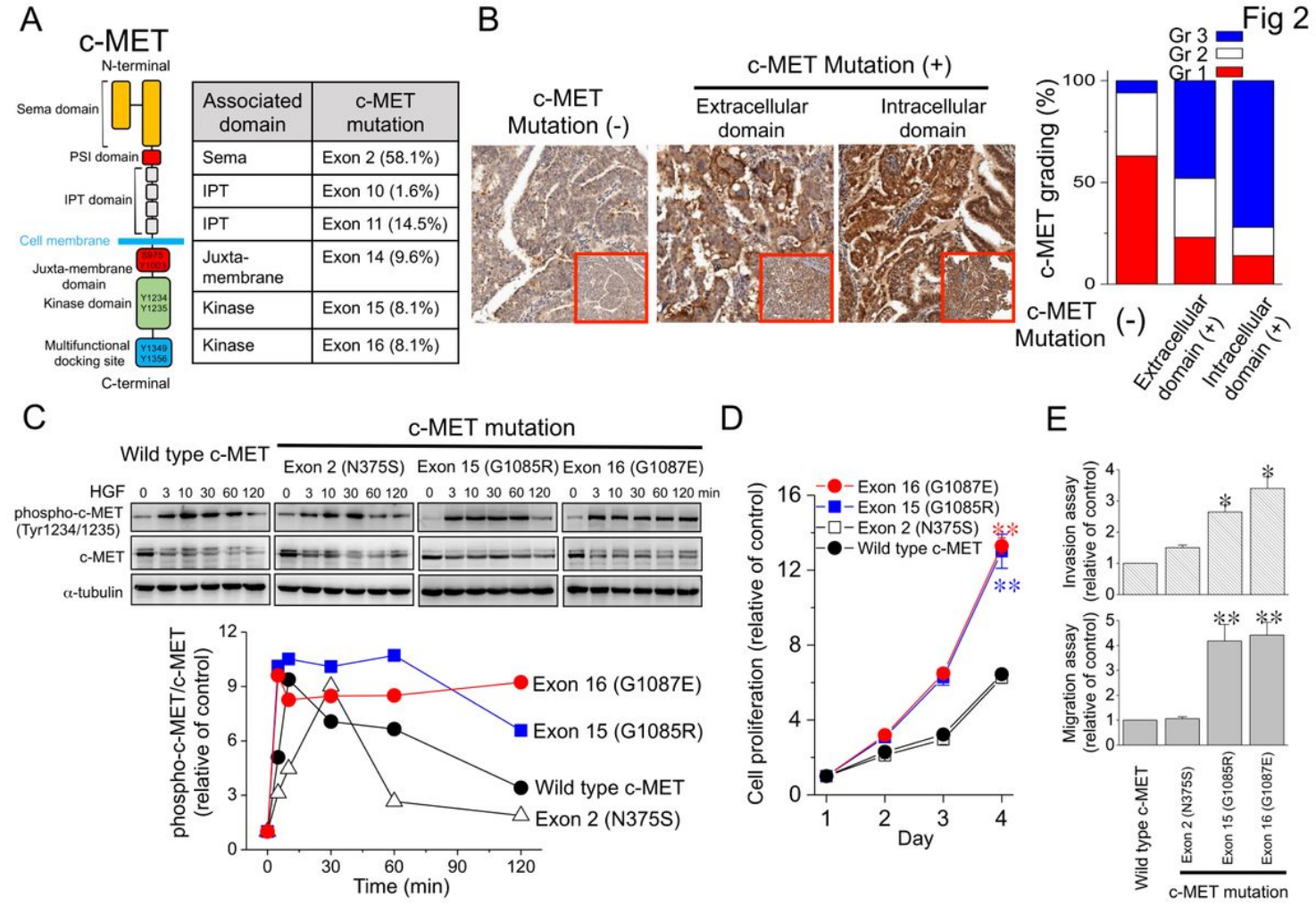

Figure 2

Differential effects of various MET mutations on c-MET phosphorylation and cellular functions. (A) The structure of c-MET (left) and distribution of MET mutations (right). Sema, semaphoring domain; PSI, plexin-semaphorin-integrin domain; IPT, immunoglobulin-plexin-transcription domain. (B) Representative images and grading of c-MET expression in endometrial cancer. The expression of c-MET was scored as grade 1–3, according to the percentage of the positively-stained tumor cells and the intensity of the staining. (C) Time course of c-MET phosphorylation in response to HGF (50 ng/ mL) stimulation. Cell lysates from various clones of the endometrial cancer RL95-2 cells were immunoblotted with anti-c-MET, anti-phospho-c-MET, and anti-α-tubulin antibodies (upper). The expression levels were quantified and the ratios of phosphor-c-MET to total c-MET are shown (bottom). (D) Cell proliferation, invasion, and migration (E) assays using various clones of the RL95-2 cells. Each value represents the mean ± standard error of mean (SEM) from at least three experiments. *, $p < 0.05$; **, $p < 0.01$.

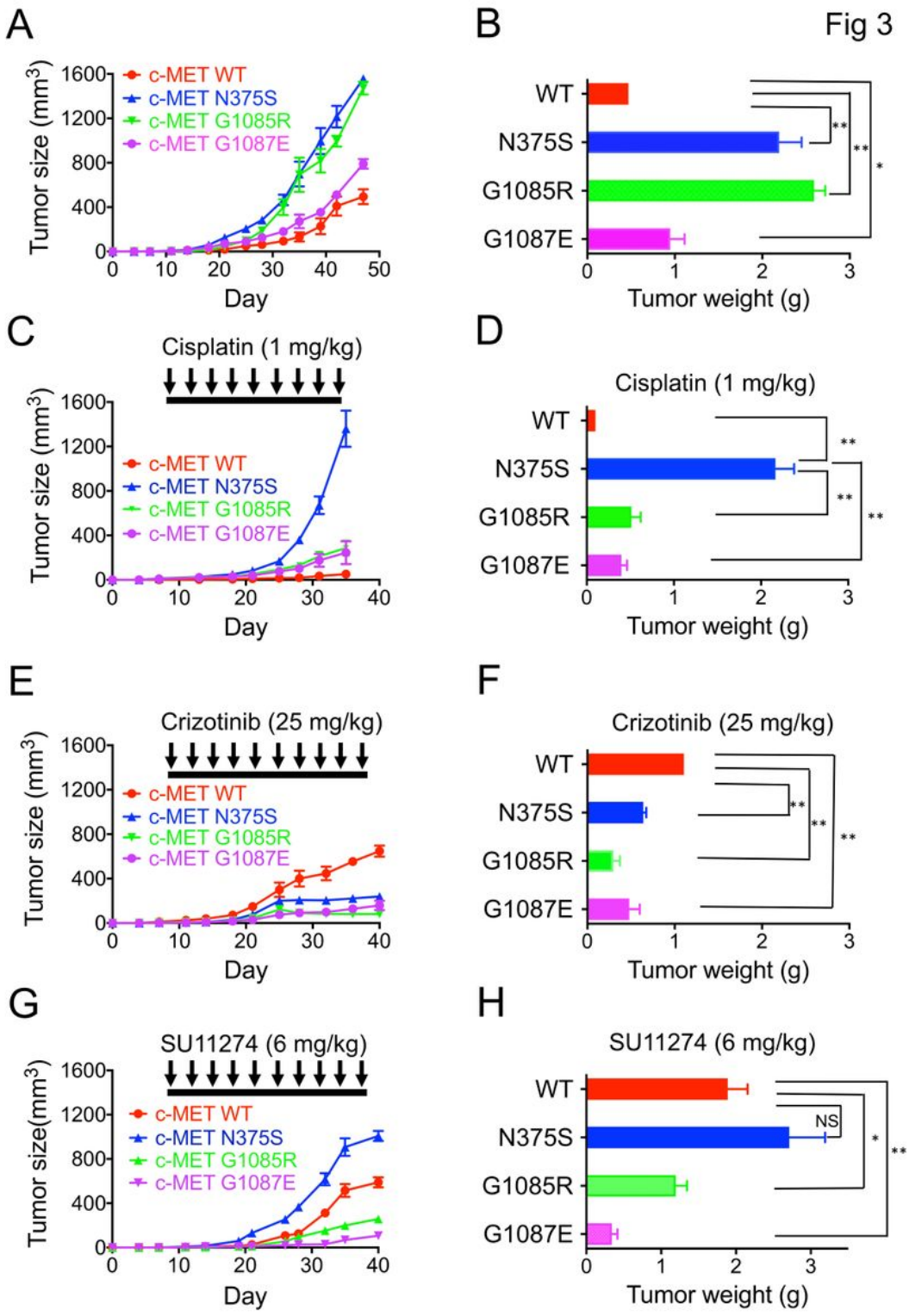

Figure 3

Antitumor effects of cisplatin and tyrosine kinase inhibitors in endometrial cancer xenografts harboring different MET mutations. 1 × 106 RL95-2 cells carrying wild-type or mutant MET, including N375S, G1085R, and G1087E, were injected into the posterior flank of SCID mice, subcutaneously. The tumors were allowed to grow and treated by observation only (A and B), cisplatin (1 mg/ kg) twice a week (C and D), crizotinib (25 mg/ kg) by oral gavage twice a week (E and F), or SU11274 (6 mg/ kg) twice a week (G

and H) (n = 5 in each treatment group). Tumor size and body weight were measured twice a week. Data are presented as the mean tumor size ± SEM. *, p < 0.05; **, p < 0.01; NS, non-significance.

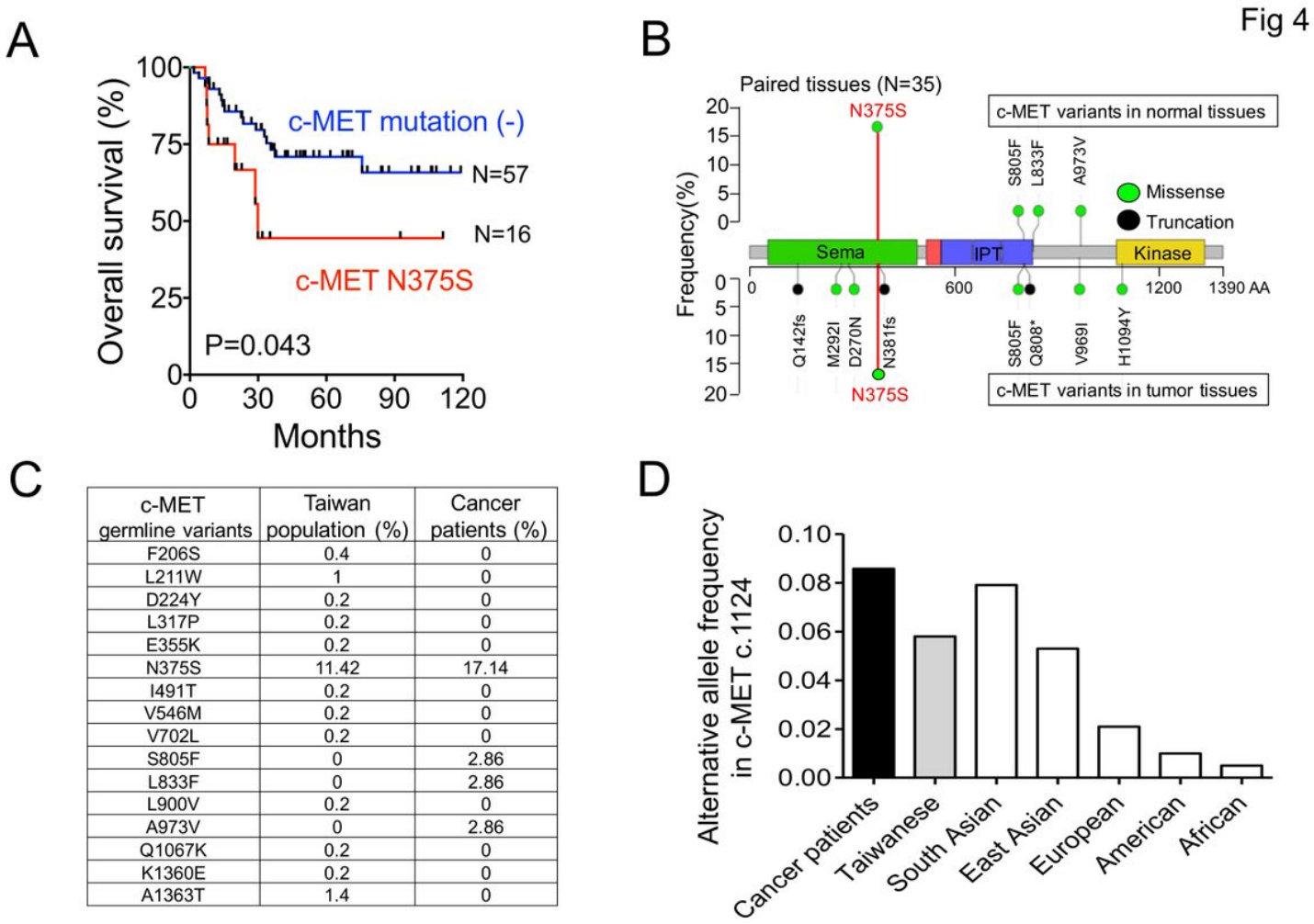

c-MET germline variants	Taiwan population (%)	Cancer patients (%)
F206S	0.4	0
L211W	1	0
D224Y	0.2	0
L317P	0.2	0
E355K	0.2	0
N375S	11.42	17.14
I491T	0.2	0
V546M	0.2	0
V702L	0.2	0
S805F	0	2.86
L833F	0	2.86
L900V	0.2	0
A973V	0	2.86
Q1067K	0.2	0
K1360E	0.2	0
A1363T	1.4	0

Figure 4

The clinical impact, distribution, and frequency of germline MET N375S variant. (A) OS of advanced endometrial cancer patients with and without the MET N375S variant. (B) The distribution and frequency of MET variants in 35 paired normal and tumor tissues. Whole-genome sequencing was used to analyze DNA extracted from blood samples or adjacent non-tumor specimens to determine germline MET variants. (C) The distribution and frequency of germline MET variants in cancer patients and the normal Taiwan population. The database from the Taiwan Biobank, which contained germline whole-genome sequencing data of 499 normal Taiwanese individuals, was used to compare the distribution and frequency of germline MET variants in the NCKUH cohort and normal Taiwan population. (D) The alternative allele frequency of MET c.1124 (N375S) in the different ethnic groups. The frequency of the variant allele in MET c.1124 was compared among the NCKUH cohort, normal Taiwanese population, and different ethnic groups enrolled in the 1,000 Genome Project.

Supplementary Files

This is a list of supplementary files associated with this preprint. Click to download.

- SupplementaryFigureS720200710.jpg
- SupplementaryFigureS620200710.jpg
- SupplementaryFigureS520200710.jpg
- SupplementaryFigureS4.jpg
- SupplementaryFigureS3.jpg
- SupplementaryFigureS2.jpg
- SupplementaryFigureS1.jpg
- SupplementaryTableS120200626.docx